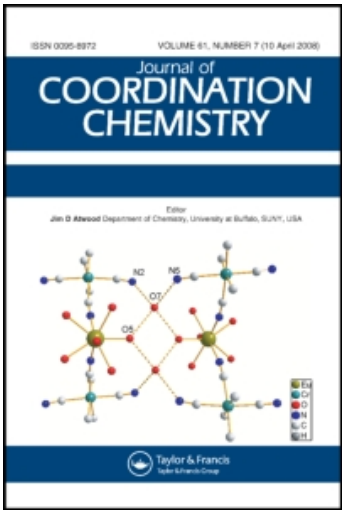


**Journal of Coordination Chemistry**
Publication details, including instructions for authors and subscription information:
http://www.informaworld.com/smpp/title~content=t713455674

# Electrochemical Investigation of Transition—Metal Complexes of the Ligand Tetrakis(2-Pyridylmethyl)-Ethylenediamine (Tpen). Crystal Structure of $[Ni(tpen)](ClO_4)_2 \cdot 2/3H_2O$

Denise Da Luz[a]; Cesar V. Franco[a]; Ivo Vencato[a]; Ademir Neves[ab]; Yvonne Primerano Mascarenhas[b]
[a] Departamento de Quimica, Universidade Federal de Santa Catarina, Florianópolis, SC, Brazil [b] Instituto de Física e Quimica de Sào Carlos, Universidade de Sào Paulo, Sào Carlos, SP, Brazil

**To cite this Article** Da Luz, Denise , Franco, Cesar V. , Vencato, Ivo , Neves, Ademir and Mascarenhas, Yvonne Primerano(1992) 'Electrochemical Investigation of Transition—Metal Complexes of the Ligand Tetrakis(2-Pyridylmethyl)-Ethylenediamine (Tpen). Crystal Structure of $[Ni(tpen)](ClO_4)_2 \cdot 2/3H_2O$', Journal of Coordination Chemistry, 26: 4, 269 — 283
**To link to this Article: DOI:** 10.1080/00958979209407929
**URL:** http://dx.doi.org/10.1080/00958979209407929

*J. Coord. Chem.* 1992, Vol. 26. pp. 269–283
Reprints available directly from the publisher
Photocopying permitted by license only



# ELECTROCHEMICAL INVESTIGATION OF TRANSITION—METAL COMPLEXES OF THE LIGAND TETRAKIS(2-PYRIDYLMETHYL)-ETHYLENEDIAMINE (TPEN). CRYSTAL STRUCTURE OF $[Ni(tpen)](ClO_4)_2.2/3H_2O$

DENISE DA LUZ, CESAR V. FRANCO, IVO VENCATO, ADEMIR NEVES*

*Departamento de Química, Universidade Federal de Santa Catarina, CEP: 88049, Florianópolis, SC, Brazil*

and YVONNE PRIMERANO MASCARENHAS

*Instituto de Física e Química de São Carlos, Universidade de São Paulo, CEP: 13560, São Carlos, SP, Brazil*

*(Received 3 May 1991; in final form 25 February 1992)*



The potentially hexadentate ligand *N,N,N',N'*-tetrakis(2-pyridylmethyl)ethylenediamine ($C_{26}H_{28}N_6$, tpen) reacts in ethanolic solution with $M(ClO_4)_2.6H_2O$ (stoichiometry 1:1; M = Mn(II), Fe(II), Co(II), Ni(II), Cu(II)) yielding the corresponding $[M(tpen)](ClO_4)_2$ complexes. The new complex $[Cr(tpen)](PF_6)_3$ was also prepared from a dimethyl sulfoxide solution of tpen and $CrCl_3.6H_2O$. The crystal structure of the violet, $[Ni(tpen)](ClO_4)_2.2/3H_2O$ complex has been determined by X-ray crystallography. Crystal data: monoclinic, space group $C2/c$; $a = 41.205(5)$, $b = 9.492(2)$, $c = 23.930(3)$ Å, $\beta = 108.02(3)°$, $V = 8{,}900(6)$ Å$^3$, $Z = 12$, $D_{cal} = 1.55\,g\,cm^{-3}$; final $R = 0.067$ from 3379 observed reflections. The structure consists of two distinct distorted octahedral Ni(II) cations, perchlorate anions and waters of crystallization. Electrochemical behaviour (cyclic voltammetry) and spectroelectrochemistry in acetonitrile shows a reversible or *quasi*-reversible one electron transfer process. The nickel(II) and copper(II) complexes can be also reduced reversibly to the corresponding (formal) nickel(I) and copper(I) complexes. Stabilization of different oxidation states is discussed in terms of the flexibility and $\pi$-acceptor capability of the ligand tpen.

**Keywords:** X-ray crystal structure, electrochemistry, tetrakis(2-pyridylmethyl)ethylenediamine, nickel(II)

## INTRODUCTION

The ligand tpen, first described by Anderegg *et al.*,[1,2] forms very stable 1:1 metal complexes with most divalent metal ions of the first transition series. In order to estimate the amount of strain that the pyridyl arms induce in the complexes, X-ray investigations of the cobalt(III) complex with this hexadentate ligand have been carried out.[3] The preparation and characterization of $[Fe(tpen)](ClO_4)_2.2/3H_2O$ as the first spin-crossover complex that interconverts between the low- and high-spin states at a rate faster than the $^{57}Fe$ Mössbauer time scale was also reported.[4] On the other hand, tpen can act as a binucleating ligand. Gagné *et al.*[5] have reported the X-ray structure of the binuclear copper(I) complex $[Cu_2(tpen)](BF_4)_2$ and its dicarbonyl adduct.[5] Recently, one of us reported the synthesis, magnetic properties

* Author for correspondence.

and crystal structure of a bis($\mu$-hydroxo) binuclear V(IV) complex with tpen, in which *syn* $\{O=V(\mu-OH)_2V=O\}^{2+}$, the first isolated V(IV) complex with this configuration, is present.[6]

In addition, heavy metal chelation by polypyridyl ligands is useful in biochemical studies. The ligand tpen has recently been used as a heavy metal chelator in studies measuring free cytosolic $Ca^{2+}$ in Ehrlich and Yoshida "Ascites Carcinomas".[7] Also, tpen has recently been used in work investigating the effect of iron chelating agents on the toxicity of dexorubicin for MCF-7 human breast cancer cells.[8]

To our surprise, no systematic investigation of electrochemical properties of the mononuclear bivalent first row transition metal complexes with the ligand tpen has been reported, except for an electrochemical investigation of $[Fe(tpen)](ClO_4)_2$.[9]

We have started a new program for systematically investigating ligands containing $\alpha$-diimine groups, which are notable for their high position in the spectrochemical series and for their ability to stabilize low valency states. The subject of this paper is cyclic voltammetric studies involving complxes of Mn(II), Fe(II), Co(II), Ni(II), Cu(II) and Cr(III) with tpen (Figure 1). Interestingly, two *quasi*-reversible one electron transfer waves in the cyclic voltammogram of $[Ni(tpen)](ClO_4)_2$ in acetonitrile have been observed, thus showing the presence of Ni(III)/Ni(II) and Ni(II)/Ni(I) species in solution. To facilitate a possible explanation for this interesting electrochemical behaviour, we have undertaken a complete crystal structural analysis of $[Ni(tpen)](ClO_4)_2.2/3H_2O$.



## EXPERIMENTAL

### *Synthesis*

The ligand *N*,*N*,*N'*,*N'*-tetrakis(2-pyridylmethyl)ethylenediamine (tpen) was prepared as described in the literature.[1,2,9] A 200 MHz NMR spectrum ($CDCl_3$) gave two single peaks and a multiplet as follows: $\delta$ 2.75 (ethylene $CH_2$), 3.75 (pyridymethyl $CH_2$), 6.9–7.8 and 8.3–8.6 (H-pyridine). The complexes $[M(tpen)[ClO_4)_2$ (M = Co, Ni, Fe, Mn and Cu) were prepared according to a general procedure described in the literature:[2] typically, tpen was added to a stirred absolute ethanolic solution containing the stoichiometric amount of the perchlorate salt of the metal. The solution was kept at 50°C for 10 min and then cooled and left overnight in a refrigerator. The crystalline products obtained were filtered off, washed with ethanol and ether, and air-dried. Electronic spectra of all complexes are in agreement with those reported in the literature.[2,4] $(Ni(tpen)](ClO_4)_2.2/3H_2O$ and $[Cu(tpen)](ClO_4)_2$ were recrystallized from hot 0.1 M $HClO_4$ Anal.: calcd. (found) for $NiC_{26}H_{28}N_6.2ClO_4$: C, 45.78

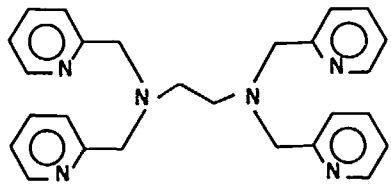


tpen

FIGURE 1 The ligand tetrakis(2-pyridylmethyl)ethylenediamine (tpen).

(45.40); H, 4.14 (4.20); N, 12.32 (12.30)% and for $CuC_{26}H_{28}N_6.2ClO_4$: C, 45.45 (46.00); H, 4.11 (4.07); N, 12.19 (12.07)%. **Caution.** The perchlorate salts are potentially dangerous; they may explode violently when heated. The complex $[Cr(tpen)](PF_6)_3$ was prepared by the following method: a solution of $CrCl_3.6H_2O$ (0.26g, 1.0 mmol) in dimethyl sulfoxide ($Me_2SO$, 20 $cm^3$) was kept in an open vessel at 150°C for 15 min until a clear green solution was obtained, to which tpen (0.42g, 1.0 mmol) ws added. The volume was reduced to approximately 7 $cm^3$ under reduced pressure and a violet microcrystalline precipitate was obtained upon addition of ethanol (*ca* 10 $cm^3$). The crystals were washed with ethanol and ether and air dried (yield: 20%). Anal.: calcd. (found) for $CrC_{26}H_{28}N_6.3PF_6$: C, 34.26 (34.10); H, 3.09 (3.15).

Crystals of $[Ni(tpen)](ClO_4)_2.2/3H_2O$ suitable for X-ray crystallography were obtained by slow evaporation of an aqueous solution of the complex. These crystals were not dried as described above and water of crystallization was found to be present.

*Electrochemistry measurements*

Electrochemical experiments were performed with a Princeton Applied Research (PAR) 273 potentiostat/galvanostat equipped with an X-Y-T recorder (ECB—Equipamentos Cientificos do Brasil). Cyclic voltammograms (CV) were measured in acetonitrile solutions containing 0.1 M tetra-*n*-butylammonium hexafluorophosphate, $[(TBA)PF_6]$ as supporting electrolyte, and were conducted at 25°C under an argon atmosphere. The electrochemical cell employed was of standard three-electrode configuration: a gold, platinum or glassy carbon working electrode, a Pt-wire auxiliary electrode, and a reference electrode (saturated calomel electrode, SCE and/or Ag/AgCl, saturated LiCl in ethanol). The performance of the reference electrode was monitored by measuring the CV of the $Fc/Fc^+$ couple. CV's were also measured in aqueous solutions containing 0.1 M $LiClO_4$ as supporting electrolyte. Half-wave potentials were taken as the average of the anodic and cathodic peak potentials of reversible (or *quasi*-reversible) cyclic voltammograms. Diagnostic criteria for reversibility of electron-transfer processes were employed in the usual manner.[10]

*Spectroelectrochemical experiments*

Optically transparent, thin layer cells were constructed according to the procedure described as follows. The transparent electrodes were a 500 wires per inch (60% transmittance) Buckbee Mears Co., gold minigrids, sandwiched between two microscope slides separated by a Teflon tape spacer. The minigrid acts as a working electrode and extended outside of the slides for electrical contact. A platinum-wire and SCE electrode were used as the auxiliary and reference electrodes, respectively. Solutions were prepared and degassed under an inert atmosphere (argon) and introduced into the cell through capillarity. The minigrid was located within 4–6 mm of the cell bottom to minimize *iR* drop. A series of potentials were sequentially applied across the gold minigrid containing a thin-layer of solution to convert the redox couple from M(II) to M(III). Each applied potential was maintained until equilibrium has been established, as defined by the Nernst equation. A Nernstian plot can then be made from the values of the applied potentials and the values of [O]/[R] (determined spectroscopically). Potentials were applied to the cell using a Bio-analytical SP-2 potentiostat/galvanostat and the spectra were recorded with a HP 8450 diode-array apparatus.

*Instrumentation*

Electronic absorption spectra in the 200–800 nm range were recorded with a Hewlett Packard HP-8450A spectrophotometer, and infra-red spectra (KBr disk) with a Perkin Elmer 781 IR spectrophotometer.

*X-ray crystallography*

A dark violet, equidimensional crystal of $[Ni(tpen)](ClO_4)_2.2/3H_2O$ was mounted on a Enraf-Nonius CAD-4 diffractometer. The cell parameters were obtained by a least-squares fit of 25 reflections ($12.8° < 2\theta < 20.9°$). Data collection was performed in the triclinic system with cell parameters $a = 9.492(2)$, $b = 21.141(10)$, $c = 23.930(5)$ Å, $\alpha = 107.55(3)°$, $\beta = 89.95(2)°$, $\gamma = 102.96(3)°$, with 10,285 integrated reflections up to $(\sin\theta)/\lambda = 0.504$ Å$^{-1}$; $w$-$2\theta$ scan technique, scan width $(0.80 + 0.35\tan\theta)°$, range of measured $hkl$ $0 < h < 9$, $-21 < k < 21$, $-24 < l < 24$; variable scan rate with maximum scan time of 20 s per reflection. No significant decrease in intensities of two standard reflections ($1, 2, \bar{1}7$ and $0\,\bar{9}\,\bar{8}$) was observed. Intensity data were corrected for Lorentz and polarization effects but no absorption correction was applied because of the low linear absorption coefficient, the favourable crystal shape, and similar intensities among equivalent reflections. The new cell in the monoclinic system was obtained with the matrix (1,2,0/1,0,0/0,0,1) giving the parameters summarized in Table I. The systematic absences were $hkl$: $h+k = 2n+1$ and $h0l$: $l = 2n+1$, consistent with the space group $C2/c$. Equivalent reflections were merged with $R_{int} = 3.6\%$.

TABLE I
Summary of crystallographic data.

| | |
|---|---|
| Formula | $C_{26}H_{28}N_6Ni(ClO_4)_2.2/3H_2O$ |
| Formula weight | 694.22 |
| Crystal system | monoclinic |
| Space group | $C2/c$ |
| $Z$ | 12 |
| $a$ (Å) | 41.205(5) |
| $b$ (Å) | 9.492(2) |
| $c$ (Å) | 23.930(3) |
| $\beta$ (°) | 108.02(3) |
| $V$ (Å) | 8900(6) |
| $D_{calc}$ (g cm$^{-3}$) | 1.55 |
| Diameter of the equant crystal | 0.50 mm |
| Temperature (°C) | 25 |
| Radiation | MoK$\alpha$ (graphite), $\lambda = 0.71073$ Å |
| Scan type | $\theta$–$2\theta$ |
| Range of measured $hkl$ | −41/39, 0/9, 0/24 |
| No. data collected | 10,285 |
| No. unique data | 4521 with 3379 ($I > 3.0\sigma(I)$) |
| Absorption coefficient (cm$^{-1}$) | 8.31 |
| Least-squares parameters | 634 |
| Parameters $k$ and $g$ in weighting scheme | 1.6868, 0.00258 |
| $R$ | 0.067 |
| $R_w$ | 0.076 |

The structure was solved with MULTAN-80[11] and successive Fourier syntheses, and refined by a least-squares procedure that utilized a 'blocked cascade" algorithm. The function minimized was $\Sigma w(|F_o|-|F_c|)^2$ with $w=k|\sigma^2(F_o)+gF_o^2|^{-1}$ where $\sigma(F_o)$ is the *esd* for the observed amplitude based on counting statistics. The positions of only 16 methyl H atoms were calculated and included in the final refinement cycle, due to the SHELX-76[12] program limitation of parameters. All non-hydrogen atoms were refined with anisotropic thermal parameters. In the final refinement cycle, maximum $(\Delta/\sigma)=0.42$ and maximum height in the final $\Delta F$ map was 0.71 e/Å$^3$, near the Ni2 atom. Scattering factors for neutral atoms were corrected for both $\Delta f'$ and $i(\Delta f'')$ terms. The calculations were carried out on an IBM/3090 computer using the SHELX-76 program package; scattering factors were taken from International Tables of X-ray Crystallography.[13]

## RESULTS AND DISCUSSION

### *Electrochemistry*

Cyclic voltammograms of $[Cr(tpen)]^{3+}$ and $[M(tpen)]^{2+}$, where M represents Co(II), Fe(II), Cu(II), Mn(II), in acetonitrile (0.1 M tetrabutylammonium hexafluorophosphate as supporting electrolyte) reveal one wave in the potential range +1.5 to −1.5 V *vs* SCE at 25°C. The peak-to-peak separation $\Delta$Ep (Table II) and $i_{p,b}/i_{p,f}$ ratio give information on electrochemical reversibility and chemical stability of the species formed on the electrode surface. Reversible or *quasi*-reversible behaviour is dominant, except for $[Mn(tpen)]^{2+}$ species, which shows an irreversible behaviour ($\Delta E_p \sim 500$ mV at scan rate of 50 mV s$^{-1}$). Formal redox potentials summarized in Table II indicate a strong stabilization of the oxidation state +3 for the chromium complex, with the reduced form being a strong reductant. This fact contrasts with electrochemical properties of the Mn(III) and Fe(III) complexes which are strong oxidants. $[Co(tpen)]^{3+}$ is a weak oxidant, with $E^{\circ\prime} = -0.12$ V *vs* $Fc^+/Fc$ in acetonitrile and $E^{\circ\prime} = +0.20$ V *vs* NHE in aqueous media (both show a reversible behaviour).

TABLE II

Formal redox potentials for $[M(tpen)]^{3+/2+}$ and $[M(tpen)^{2+/+}$ couples at 22°C (*vs* ferrocenium/ferrocene).[a]

| Couple | E°′, V | ΔEp[b], mv | ip, b/ip, f[d] | Electrode | Reversibility |
|---|---|---|---|---|---|
| $[Cr(tpen)]^{3+/2+}$ | −1.34 | 90 | 0.80 | gold | qr |
| $[Mn(tpen)]^{3+/2+}$ | +0.70 | ≃500 | — | glassy carbon | irr |
| $[Fe(tpen)]^{3+/2+}$ | +0.38 | 60 | 1.0 | platinum | rev. |
| $[Co(tpen)]^{3+/2+}$ | −0.12 | 60 | 0.9 | gold | rev. |
| $[Co(tpen)]^{3+/2+}$ | +0.20[c] | 65 | 1.0 | platinum | rev. |
| $[Ni(tpen)]^{3+/2+}$ | +1.18 | 90 | 0.6 | glassy carbon | qr. |
| $[Ni(tpen)]^{2+/+}$ | −1.88 | 70 | 0.80 | glassy carbon | rev. |
| $[Cu(tpen)]^{2+/+}$ | −0.60 | 60 | 0.93 | glassy carbon | rev. |

[a] Measured in $CH_3CN$ with 0.1 M tetrabutylammonium hexafluorophosphate as supporting electrolyte; $10^{-3}$ M ferrocene. [b] Separation between the anodic and cathodic peaks of the cyclic voltammogram at a scan rate of 50 mV. [c] Measured in water with 0.1 M lithium perchlorate as supporting electrolyte, E°′ *vs* NHE; key: qr, *quasi*-reversible; rev, reversible, irr, irreversible. [d] b = back-reaction, f = forward reaction.

It is interesting to note that $[Cu(tpen)]^{2+}$ also exhibits reversible charge transfer behaviour with E°′ of −0.60 V *vs* $Fc^+/Fc$, ΔEp = 60 mV and an $i_{p,b}/i_{p,f}$ ratio of 0.93 for the $[Cu(tpen)]^{2+/+}$ couple. Coulometric measurements of $[Cu(tpen)]^{2+}$ at −1.10 V *vs* $Fc^+/Fc$ reveal that this species is reduced by 1.0±0.2 electrons for each copper site. Cyclic voltammograms (CV) of this solution show the same value of heterogeneous electron transfer under the same conditions. From this information, we suggest that Cu(I) could be formed in solution without changing the coordination sphere at the copper centre. Based on infra-red spectroscopy, Anderegg *et al.*[2] proposed that in the complex $[Cu(tpen)]^{2+}$ the ligand is in its pentacoordinated form with a pendant pyridyl arm. An X-ray structural characterization of $[Cu(tpen)](ClO_4)_2$ is in progress in our laboratory and will be reported separately.

CV studies involving $[Fe(tpen)]^{2+}$ in acetonitrile (0.1 M $TBA(PF_6)$ as supporting electrolyte) show electrochemical behaviour in complete agreement with data published in the literature.[9] Cyclic voltammograms of $[Fe)tpen)]^{2+}$ in aqueous solution (0.1 M $Na_2SO_4$ as supporting electrolyte) were performed in the potential range from 0.0 to +0.80 V *vs* SCE. The CV reveals one *quasi*-reversible one electron wave at 0.26 V which is attributed to the $[Fe(tpen)]^{3/2+}$ couple. Coulometric measurements of $[Fe(tpen)]^{2+}$ in aqueous solution at −0.6 V *vs* SCE revealed that this species is oxidized by 1.0±0.1 electron for each iron site. The CV shows the same value of heterogeneous electron transfer under the same conditions. In order to measure the E°′ value and the electron stoichiometry of the $[Fe(tpen)]^{3+/2+}$ couple as well as the electronic spectra of the oxidized $[Fe(tpen)]^{3+}$ species, spectropotentiostatic experiments were performed under the same experimental conditions as employed in the CV studies. Figure 2A shows potential-dependent spectral changes due to electrolysis of a $2.0\times10^{-4}$ M solution of $[Fe(tpen)]^{2+}$ in aqueous solution (0.1 M $Na_2SO_4$). The maintenance of a strict isobestic point in successive spectra supports constant stoichiometry throughout the course of the electrolysis. Data for the Nernst plot shown in Figure 2B were obtained by recording absorbance at 416 nm after equilibrium was established, following selected potential steps. The (E°′ = 0.29 V *vs* SCE and $n = 0.84$ electron) values obtained from this plot are in excellent agreement with the CVs and coulometric results. $[Fe(tpen)]^{3+}$ exhibits a shoulder at 416 nm.

Finally, the cyclic voltammogram of $[Ni(tpen)]^{2+}$ was recorded from 2.0 V to −1.6 V *vs* Ag/AgCl in acetonitrile using $TBAPF_6$ as supporting electrolyte (Figure 3). The resulting voltammogram shows both a reversible, one electron wave, E°′ = −1.88 V *vs* $Fc^+/Fc$, corresponding to the formation of $[Ni(tpen)]^+$, and a *quasi*-reversible one electron wave, E°′ = 1.15 V *vs* $Fc^+/Fc$, corresponding to the formation of $[Ni(tpen)]^{3+}$. Voltammetric data are consistent with the reaction below.

$$[Ni(tpen)]^+ \underset{+e}{\overset{-e}{\rightleftharpoons}} [Ni(tpen)]^{2+} \underset{+e}{\overset{-e}{\rightleftharpoons}} [Ni(tpen)]^{3+}$$

Cyclic voltammograms for $[Ni(tpen)]^{2+/+}$ and $[Ni(tpen)]^{+3/+2}$ were recorded independently in order to confirm the reversibility of $[Ni(tpen)]^{2+/+}$ and *quasi*-reversibility of $[Ni(tpen)]^{3+/2+}$ couples. A cyclic voltammogram was recorded in the potential range −0.6 V to −1.6 V *vs* Ag/AgCl, at scan rates from 20 to 500 mV $s^{-1}$. The resulting CV displays a peak-to-peak separation, $\Delta E_P = 60$ mV, and an $i_{p,b}/i_{p,f}$ ratio of 0.80 V, remaining constant even at high scan rates, as expected for the $[Ni(tpen)]^{2+/+}$ couple. Controlled potential coulometry, at −2.0 V *vs* $Fc^+/Fc$, revealed a one electron reduction of $[Ni(tpen)]^{2+}$. We must emphasize here that, as

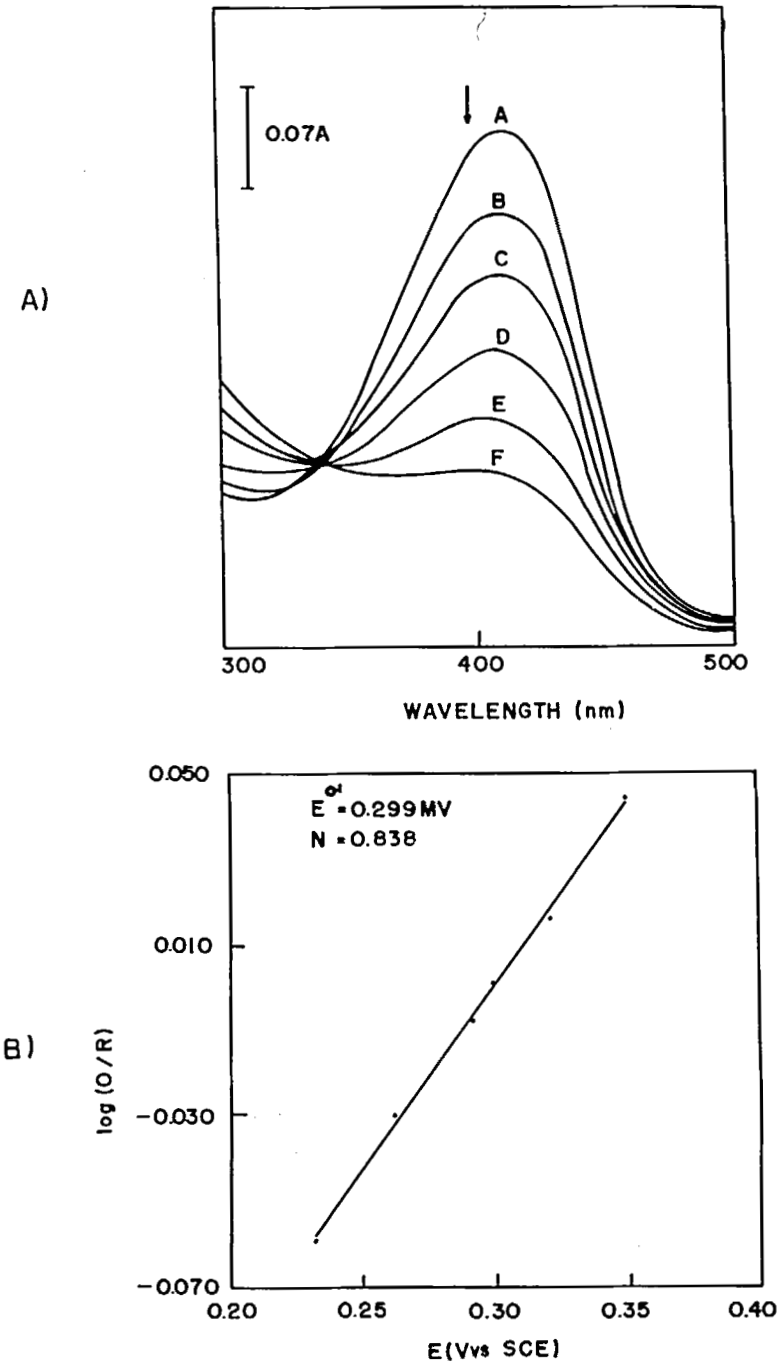


FIGURE 2 A: Spectra recorded during spectropotentiostatic experiments on 0.2 mM $[Fe(tpen)]^{2+}$ in aqueous solution (0.1 M $Na_2SO_4$). Applied potentials in mV *vs* SCE are as follows: (A) 20, (B) 23, (C) 26, (D) 29, (E) 32, (F) 35. B: Nernst plot of data from Figure 2A at 416 nm.

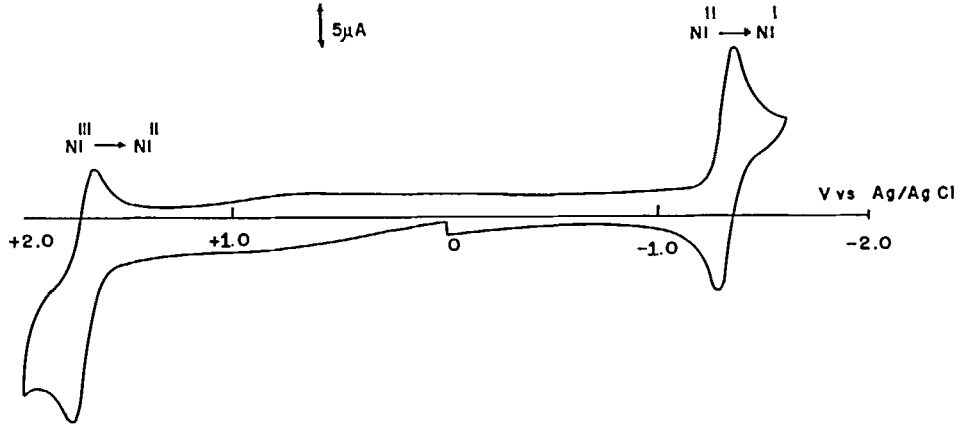


FIGURE 3 Cyclic voltammogram of $[Ni(tpen)]^{2+}$ in acetonitrile (0.1 M $(TBA)PF_6$) at 25° (glassy-carbon working electrode, scan rate $50\,mV\,s^{-1}$).



with the case of the Cu(I) complex, Ni(I) probably is formed in solution without change of coordination sphere. On the other hand, the $[Ni(tpen)]^{3+/2+}$ couple displays a *quasi*-reversible CV wave in the range 1.95 V to 1.45 V *vs* Ag/AgCl, as is evident from the adherence to the following criteria: (i) The $E^{\circ\prime}$ values ($E^{\circ\prime}=0.5(E_{Pa}+E_{Pc})$) are independent of scan rates ($10\,mV\,s^{-1}$ to $500\,mV\,s^{-1}$); (ii) the separation of peak potentials ($\Delta E_P=E_{Pc}-E_{Pa}$) increases with scan rate and is greater than 60 mV even at low scan rates. From these results, it is apparent that $[Ni(tpen)]^{+}$ is more easily formed, electrochemically. However, from the $i_{p,b}/i_{p,f}$ value of Figure 3 it is clear that $[Ni(tpen)]^{3+}$ is not so chemically stable. In fact, the stability of the reduced form of this complex on the time scale of the coulometric measurement may be interpreted in terms of the flexibility and adaptability of the ligand tpen to changes of geometry in the first coordination sphere, caused during change of the formal oxidation states. This fact is strongly corroborated by the X-ray structure determination of the $[Ni(tpen)]^{2+}$ ion which shows a very distorted structure. In addition to this effect, stabilization of the reduced form of Ni(I) and Cu(I) is evident from the $\pi$-acceptor capability of the four pyridine rings. The consistency of this interpretation can be inferred from the strong field nature of tpen. The magnitude of *Dq* for $[Ni(tpen)]^{2+}$ ($1216\,cm^{-1}$) is only $49\,cm^{-1}$ lower than that for the tris(bipyridyl) complex[14] and $54\,cm^{-1}$ lower than that for the tris(1,10-phenantroline) complex.[14] However, these effects are not as dramatic as expected, and hence the failure to isolate the Ni(I) species causes no surprise. Figure 4 shows the redox potentials as a function of the number of *d* electrons for first-row transition metal complexes of $(edta^{4-})$[15] and tpen. Potentials of complexes containing $edta^{4-}$ are in all cases more negative (by 150 to 650 mV) than $[M(tpen)]^{3+/2+}$ couples. The $\pi$-acceptor feature of tpen causes the stabilization of the +2 oxidation state. The $[Co(tpen)]^{3+/2+}$ couple is an exception, since it shows a 90 mV negative shift relative to the $[Co(edta)]^{-/2-}$ couple. This probably occurs because the ligand acts as a pentadentate towards Co(II)[16] while tpen is hexacoordinated in the Co(III) and Co(II) species.[2,3] The resulting plot relating the redox potentials for the couples $[M(tpen)]^{3+/2+}$ with first-row transition-metal ions (Figure 4) clearly indicates the weak $\pi$-acceptor capability of

the hexadentate tpen ligand with its four pyridine rings, a feature which is more pronounced for the iron(II) complex. Similar behaviour has been observed by Wieghardt *et al.*[17] for the complexes $[M(tacn)_2]^{3+/2+}$ and $[ML]^{3+/2+}$, containing the pure $\sigma$-donor ligand tacn = 1,4,7-triazacyclononane and the weak $\pi$-acceptor ligand L = 1,4,7-tris(2-pyridylmethyl)-1,4,7-(triazacyclononane). Redox potentials of metal complexes containing the pure $\sigma$-donor ligand are in all cases more negative (by 400 mV) than those of $[ML]^{3+/2+}$ couples containing the ligand with the $\pi$-acceptor pyridyl arms.[17]

*Description of the structure of* $[Ni(tpen)]^{2+}$

The structure consists of two distinct dications containing Ni, three non-coordinating disordered perchlorate anions and waters of crystallization. Atomic parameters and selected interatomic distances and angles are given in Tables III and IV. See also Supplementary Material.

Molecule 1 lies on a crystallographic two-fold axis which passes throughout the central atom Ni1, and the dication in a general position is designated as molecule 2. The atom labelling scheme for 1 is shown in Figure 5, where the primes are used to represent symmetry related atoms by $-x, y, 1.5-z$. Molecule 2 is shown in Figure 6. The drawings were made with ORTEP.[18]



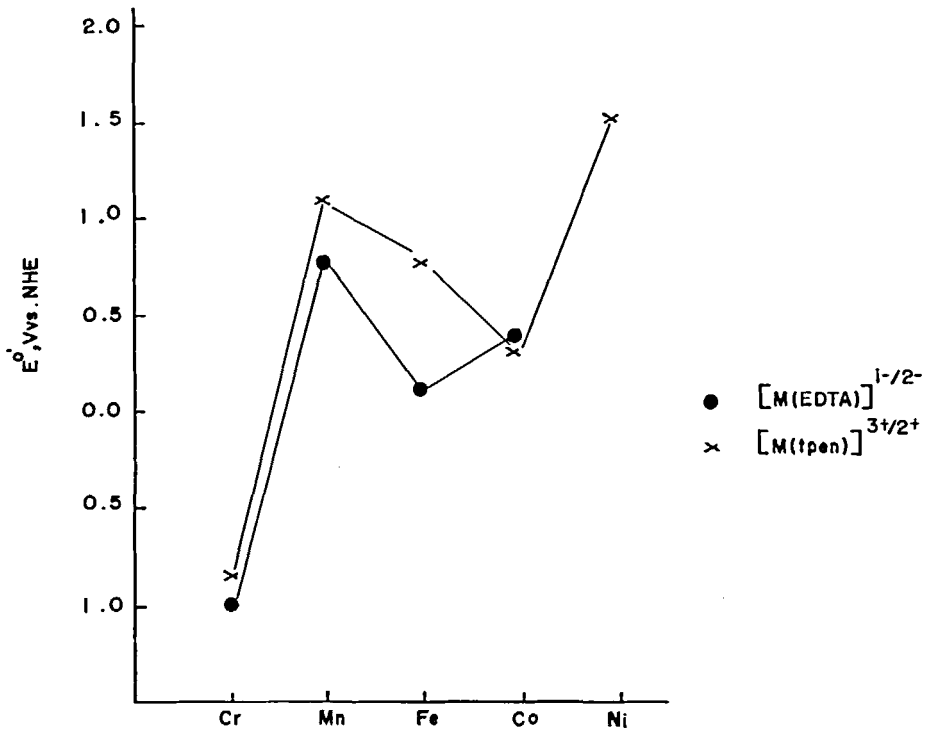


FIGURE 4 Redox potentials (V *vs* NHE) for the couples $[M(tpen)]^{3+/2+}$ and $[M(edta]^{-/2-}$ (values taken from ref. 19). Lines are drawn only as a guide.

TABLE III
Atomic parameters for Ni[tpen]$(ClO_4)_2.2/3H_2O$.

| Atom | *x/a* | *y/b* | *z/c* | $B^*_{eq}$(Å$^2$) |
|---|---|---|---|---|
| Ni1 | 0.0000$^+$ | 0.1779(1) | 0.7500$^+$ | 2.15(4) |
| N11 | −0.0072(2) | 0.1744(7) | 0.6602(3) | 4.0(2) |
| N21 | −0.0358(2) | 0.0122(6) | 0.7267(3) | 4.9(2) |
| N31 | −0.0443(2) | 0.2953(7) | 0.7360(3) | 4.2(2) |
| C011 | −0.0307(2) | 0.0815(9) | 0.6295(4) | 5.0(3) |
| C021 | −0.0380(3) | 0.060(1) | 0.5686(4) | 6.1(4) |
| C031 | −0.0218(3) | 0.141(1) | 0.5399(4) | 6.5(4) |
| C041 | 0.0026(2) | 0.245(1) | 0.5697(4) | 5.8(3) |
| C051 | 0.0083(2) | 0.2584(9) | 0.6296(3) | 4.9(3) |
| C061 | −0.0711(2) | 0.212(1) | 0.7382(4) | 5.1(3) |
| C071 | −0.1027(3) | 0.263(1) | 0.7313(5) | 7.5(5) |
| C081 | −0.1077(3) | 0.407(2) | 0.7218(6) | 9.1(5) |
| C091 | −0.0811(3) | 0.497(1) | 0.7190(5) | 7.9(4) |
| C101 | −0.0483(2) | 0.4345(9) | 0.7269(4) | 5.2(3) |
| C111 | −0.0635(2) | 0.060(1) | 0.7512(4) | 5.9(3) |
| C121 | −0.0505(2) | −0.0006(9) | 0.6611(3) | 5.5(3) |
| C131 | −0.0169(2) | −0.1140(8) | 0.7545(4) | 6.0(3) |
| Ni2 | 0.1677(0) | 0.7583(1) | 0.5944(0) | 2.38(3) |
| N12 | 0.1416(2) | 0.9527(7) | 0.5871(3) | 4.4(2) |
| N22 | 0.1337(2) | 0.7044(7) | 0.6401(3) | 4.8(2) |
| N32 | 0.1275(2) | 0.6947(7) | 0.5243(3) | 4.3(2) |
| N42 | 0.1916(2) | 0.5602(7) | 0.5935(3) | 4.7(2) |
| N52 | 0.2041(2) | 0.7694(6) | 0.6780(3) | 4.5(2) |
| N62 | 0.2078(1) | 0.8542(6) | 0.5726(3) | 4.2(2) |
| C012 | 0.1132(2) | 0.9454(8) | 0.6049(3) | 4.4(3) |
| C022 | 0.0880(2) | 1.0467(9) | 0.5886(4) | 4.8(3) |
| C032 | 0.0910(2) | 1.155(1) | 0.5537(4) | 5.6(3) |
| C042 | 0.1193(2) | 1.1643(9) | 0.5345(4) | 5.8(3) |
| C052 | 0.1448(2) | 1.0593(9) | 0.5535 | 5.2(3) |
| C062 | 0.1049(2) | 0.6136(9) | 0.5413(3) | 4.5(3) |
| C072 | 0.0774(2) | 0.551(1) | 0.5010(4) | 5.6(3) |
| C082 | 0.0732(2) | 0.569(1) | 0.4411(5) | 7.0(4) |
| C092 | 0.0954(2) | 0.656(1) | 0.4248(4) | 6.1(3) |
| C102 | 0.1214(2) | 0.719(1) | 0.4668(4) | 5.4(3) |
| C112 | 0.1141(2) | 0.5820(9) | 0.6053(4) | 5.5(3) |
| C122 | 0.1111(2) | 0.825(1) | 0.6423(4) | 5.8(3) |
| C132 | 0.1553(2) | 0.6631(9) | 0.7000(3) | 5.0(3) |
| C142 | 0.2213(2) | 0.5491(8) | 0.6368(4) | 4.7(3) |
| C152 | 0.2461(3) | 0.447(1) | 0.6374(5) | 6.7(4) |
| C162 | 0.2384(3) | 0.351(1) | 0.5915(6) | 7.1(4) |
| C172 | 0.2065(3) | 0.3596(9) | 0.5486(5) | 6.3(4) |
| C182 | 0.1846(2) | 0.4636(9) | 0.5497(4) | 5.4(3) |
| C192 | 0.2318(2) | 0.9095(8) | 0.6205(3) | 4.6(3) |
| C202 | 0.2604(2) | 0.9753(9) | 0.6160(4) | 5.5(3) |
| C212 | 0.2654(2) | 0.982(1) | 0.5626(5) | 6.3(4) |
| C222 | 0.2419(2) | 0.925(1) | 0.5135(4) | 5.7(3) |
| C232 | 0.2134(2) | 0.8603(9) | 0.5197(3) | 4.7(3) |
| C242 | 0.2222(2) | 0.9010(8) | 0.6772(3) | 5.0(3) |
| C252 | 0.2281(2) | 0.6494(9) | 0.6864(4) | 6.1(3) |

TABLE III—*continued*

| *Atom* | *x/a* | *y/b* | *z/c* | $B^*_{eq}$(Å$^2$) |
|---|---|---|---|---|
| C262 | 0.1846(2) | 0.7673(8) | 0.7192(3) | 5.2(3) |
| Cl1 | 0.1795(1) | 0.2482(2) | 0.7178(1) | 5.09(7) |
| O11 | 0.2069(2) | 0.2377(8) | 0.6937(4) | 9.5(4) |
| O21 | 0.1747(2) | 0.1178(7) | 0.7401(3) | 8.8(3) |
| O31 | 0.1493(2) | 0.2928(9) | 0.6755(3) | 9.4(3) |
| O41 | 0.1875(2) | 0.3497(8) | 0.7627(3) | 8.5(3) |
| Cl2 | 0.0088(1) | 0.6767(2) | 0.6064(1) | 5.21(8) |
| O12 | −0.0033(6) | 0.636(2) | 0.6508(7) | 6.2(5) |
| O22 | 0.0296(5) | 0.791(2) | 0.615(1) | 9.8(9) |
| O32 | 0.0268(6) | 0.576(2) | 0.590(1) | 10.7(8) |
| O42 | −0.0226(4) | 0.704(2) | 0.5578(8) | 9.8(7) |
| O12′ | −0.018(2) | 0.685(6) | 0.634(2) | 20.0(1) |
| O22′ | 0.0217(8) | 0.819(3) | 0.6116(9) | 3.5(6) |
| O32′ | 0.0384(7) | 0.607(3) | 0.643(2) | 13.0(1) |
| O42′ | −0.0025(9) | 0.609(4) | 0.5553(8) | 10.0(1) |
| Cl3 | 0.1502(1) | 0.7979(4) | 0.8738(2) | 8.6(1) |
| O13 | 0.1245(4) | 0.818(2) | 0.8264(8) | 22.5(9) |
| O23 | 0.1387(6) | 0.698(2) | 0.9059(8) | 26.0(1) |
| O33 | 0.1738(4) | 0.748(3) | 0.8577(9) | 31.0(1) |
| O43 | 0.1604(8) | 0.893(3) | 0.9124(8) | 35.0(1) |
| OW | 0.1819(3) | 0.182(1) | 0.8792(4) | 14.5(5) |

[+] Fixed to place it on the 2-fold axis. * $B_{eq}=4/3\sum_i\sum_j B_{ij}(a_i.a_j)$.



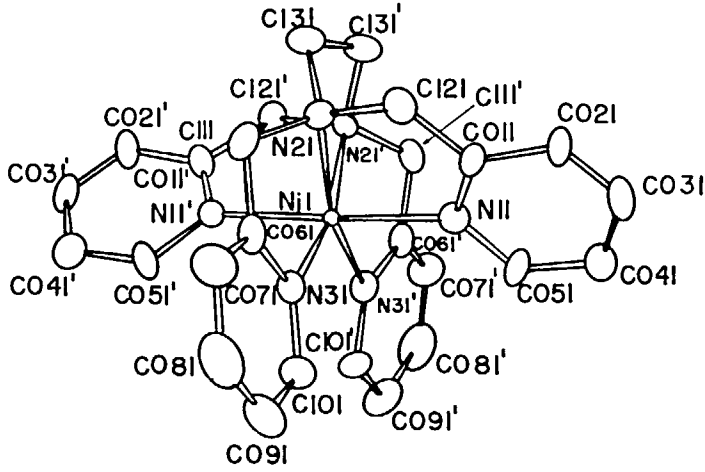


FIGURE 5 Perspective view of molecule 1 of Ni[tpen]$(ClO_4)_2.2/3H_2O$ on the crystallographic two-fold axis with atom labelling scheme (H atoms omitted).

TABLE IV
Selected bond distances (Å) and angles (°) for $Ni[tpen](ClO_4)_2.2/3H_2O$.

| | | | |
|---|---|---|---|
| | | *Molecule 1* | |
| Ni1–N11 | 2.076(6) | N31–CO61 | 1.372(12) |
| Ni1–N21 | 2.110(7) | N31–C101 | 1.341(11) |
| Ni1–N31 | 2.077(7) | N11'–CO11' | 1.347(10) |
| Ni1–N11' | 2.076(6) | N11'–CO51' | 1.367(12) |
| Ni1–N21' | 2.110(7) | N21'–C111' | 1.505(13) |
| Ni1–N31' | 2.076(7) | N21'–C121' | 1.503(10) |
| N11–CO11 | 1.347(10) | N21'–C131' | 1.472(10) |
| N11–CO51 | 1.367(12) | N31'–CO61' | 1.372(12) |
| N21–C111 | 1.505(13) | N31'–C101' | 1.341(11) |
| N21–C121 | 1.503(10) | | |
| N21–C131 | 1.472(10) | | |
| N11–Ni1–N21 | 81.4(3) | N21–Ni1–N31' | 162.0(3) |
| N11–Ni1–N31 | 90.2(2) | N31–Ni1–N11' | 90.7(3) |
| N11–Ni1–N11' | 178.2(3) | N31–Ni1–N21' | 162.0(3) |
| N11–Ni1–N21' | 97.2(3) | N21–Ni1–N31' | 115.1(3) |
| N11–Ni1–N31' | 90.7(3) | N11'–Ni1–N21' | 81.4(3) |
| N21–Ni1–N31 | 81.3(3) | N11'–Ni1–N31' | 90.2(2) |
| N21–Ni1–N11' | 97.2(3) | N21'–Ni1–N31' | 81.3(3) |
| N21–Ni1–N21' | 83.6(3) | | |
| | | *Molecule 2* | |
| Ni2–N12 | 2.116(6) | N32–CO62 | 1.363(11) |
| Ni2–N22 | 2.091(8) | N32–C102 | 1.340(11) |
| Ni2–N32 | 2.050(6) | N42–C142 | 1.343(10) |
| Ni2–N42 | 2.126(7) | N42–C182 | 1.353(11) |
| Ni2–N52 | 2.099(6) | N52–C242 | 1.459(10) |
| Ni2–N62 | 2.089(7) | N52–C252 | 1.480(11) |
| N12–CO12 | 1.363(12) | N52–C262 | 1.455(13) |
| N12–CO52 | 1.324(11) | N62–C192 | 1.366(9) |
| N22–C112 | 1.511(10) | N62–C232 | 1.356(11) |
| N22–C122 | 1.481(12) | | |
| N22–C132 | 1.487(10) | | |
| N12–Ni2–N22 | 81.4(3) | N22–Ni2–N62 | 161.3(3) |
| N12–Ni2–N32 | 85.9(2) | N32–Ni2–N42 | 89.5(2) |
| N12–Ni2–N42 | 174.8(2) | N32–Ni2–N52 | 162.3(3) |
| N12–Ni2–N52 | 103.3(2) | N32–Ni2–N62 | 115.2(3) |
| N12–Ni2–N62 | 91.1(3) | N42–Ni2–N52 | 81.8(2) |
| N22–Ni2–N32 | 81.6(3) | N42–Ni2–N62 | 88.8(3) |
| N22–Ni2–N42 | 100.2(3) | N52–Ni2–N62 | 80.1(3) |

Ni2 lies in a strongly distorted octahedral site; two pyridine and two aliphatic nitrogen atoms of the ethylenediamine "backbone" form the equatorial plane, where the nitrogen atoms of the same nature occupy the *cis* positions with respect to each other. The remaining pyridine nitrogen atoms are in axial positions with an angle N12–Ni2–N42 of 174.8°. The mean bond distances between Ni2 atom and $N_{py}$ atoms of the equatorial plane and $N_{py}$ atoms of the axial positions are very different (2.069

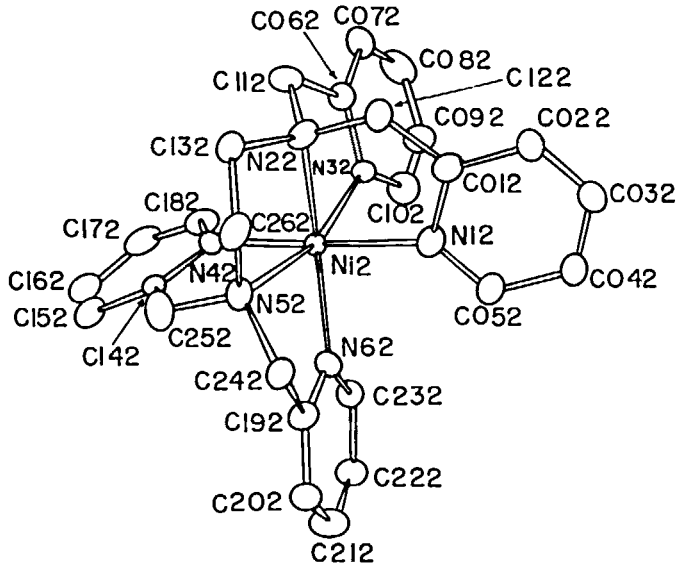


FIGURE 6 Perspective view of molecule 2 of Ni[tpen]$(ClO_4)_2.2/3H_2O$ with atom labelling scheme (H atoms omitted).



and 2.121 Å, respectively) in contrast with the values of 2.090 Å in $Ni(phen)_3^{2+}$ [19] and 2.089 Å in $Ni(bipy)_3^{2+}$.[20] Probably, this is due to steric repulsion between the pyridine rings N12–C012–C022–C032–C042–C052 and N32–C062–C072–C082–C092–C102, whose dihedral angle given by least-squares planes is 72.3°, and also between the pyridine rings N42–C142–C152–C162–C172–C182 and N62–C192–C202–C212–C222–C232, with an angle of 69.5°.

Ni1 has a less distorted octahedral coordination geometry than Ni2. Bond distances between the Ni1 atom and the pyridine nitrogen atoms are similar, with a mean value of 2.076 Å, but the Ni1–N21 ($N21 = N_{aliph}$) distance of 2.110 Å is in relatively good agreement with that (2.124 Å) found in $Ni(en)_3^{2+}$.[21]

The strain in $[Ni(tpen)]^{2+}$ is great enough to distort both octahedra in opposite senses. The N–Ni–N angles in the faces N12–N22–N32 and N42–N52–N62 are all acute. As expected, the N–Ni–N angles outside of these faces are all obtuse. An interesting measure of the overall strain in 1 and 2 is given by the angles N31–Ni1–N31′ = 114.9° and N32–Ni2–N62 = 115.2°. These angles are in the plane of, and opposite to, the ethylenediamine ring and are the most strained angles in both octahedra.

The rigidity of the pyridyl arms causes ring strain in the relatively planar chelate rings containing pyridine nitrogen atoms. An analysis of the torsion angles within the two ring arms in the equatorial plane gives the extent of puckering in the inner and the outer regions of these chelate rings for the Ni2 molecule. The angles are N32–Ni2–N22–C112 = 33.5° and Ni2–N32–C062–C112 = −2.5°: N62–Ni2–N52–C242 = 35.0° and Ni2–N62–C192–C242 = −5.5°. The corresponding angles for the Ni1 molecule are N31–Ni1–N21–C111 = −33.8° and Ni1–N31–C061–C111 = 1.5°. The ethylenediamine backbone of molecules 1 and 2 have torsion angles N21–C131–

C131'–N21' and N22–C132–C262–N52 of 60.9° and −57.8°, respectively, with the usual *gauche* configuration.[22] The five-membered rings Ni1–N21–C131–C131'–N51 and Ni2–N22–C132–C262–N52 cannot deviate greatly from planarity due to ring strain.

The $[Cl(1)O_4]^-$ counterion shows normal tetrahedral coordination, but each of the four oxygen atoms of $[Cl(2)O_4]^-$ anion assumes two positions, the population parameters of these sites being 0.59 and 0.41. These disordered oxygen atoms were refined anisotropically. Thermal vibrational parameters of the four oxygen atoms of the $[Cl(3)O_4]^-$ anion are very large and clearly anisotropic, thus indicating possible positional disorder. No attempt was made to analyze these atomic thermal parameters in terms of molecular rigid body motion.

The water molecule OW, is linked to the oxygen perchlorate atoms 043 $(x, 1-y, z)$ and 021 through weak hydrogen bonds suggested by the distances and angle 3.06 Å, 3.31 Å and 98.0°, respectively.

ACKNOWLEDGEMENTS

We are grateful to the Conselho Nacional de Desenvolvimento Cientifico e Tecnológico (CNPq), contract 405095/88-QU, Fundação de Amparo a Pesquisa do Estado de São Paulo (FAPESP) and Financiadora de Estudos e Projetos (FINEP). We thank Dr Phalguni Chaudhuri and Dr Manfredo Hörner for helpful discussions.



## SUPPLEMENTARY MATERIAL

Full lists of hydrogen parameters, anisotropic thermal parameters, bonding details and observed and calculated structure factors are available from the author on request.

REFERENCES

1. G. Anderegg and F. Wenk, *Helv. Chim. Acta*, **50**, 2330 (1967).
2. G. Anderegg, E. Hubmann, N.G. Podder and F. Wenk, *Helv. Chim. Acta*, **60**, 123 (1970).
3. J.B. Mandel and B.E. Douglas, *Inorg. Chim. Acta*, **155**, 55 (1989).
4. (a) H. Toftlund and S. Yde-Andersen, *Acta Chem. Scand.*, **A35**, 575 (1981); (b) H.R. Chang, J.K. McCuster, H. Toftlund, S.D. Wilson, A.X. Trautwein, H. Winkler and D.N. Hendrickson, *J. Am. Chem. Soc.*, **112**, 6814 (1990).
5. R.R. Gagné, R.P. Kreh, J.A. Dodge, R.E. Marsh and M. McCool, *Inorg. Chem.*, **21**, 254 (1982).
6. A. Neves, K. Wieghardt, B. Nuber and J. Weiss, *Inorg. Chim. Acta*, **150**, 183 (1988).
7. P. Arslan, F. Divirgilio, M. Beltrame, R.Y. Tsien and T. Pozzan, *J. Biol. Chem.*, **260**, 2719 (1985).
8. J.H. Doroshow, *Biochem. Biophys. Res. Commun.*, **135**, 330 (1986).
9. R.K. Boggess, J.W. Hughes, C.W. Chew and J.J. Kemper, *J. Inorg. Nucl. Chem.*, **43**, 939 (1981).
10. R.S. Nicholson and I. Shain, *Anal. Chem.*, **36**, 706 (1964).
11. P. Main, S.J. Fiske, S.E. Hull, L. Lessinger, G. Germain, J.P. Declercq and M.M. Woolfson, "MULTAN-80. A System of Computer Programs for Automatic Solution of Crystal Structures from X-ray Diffraction Data", (Universities of York, England and Louvain, Belgium, 1980).
12. G.M. Sheldrick, "SHELX-76. Programme for Crystal Structure Determination" (University of Cambridge, England, 1976).
13. International Tables for X-Ray Crystallography, Vol. IV, Kynock Press, Birmingham, U.K., 1974.
14. S.M. Nelson and J. Rodger, *J. Chem. Soc. (A)*, 272 (1968).
15. H. Ogino, T. Nagata and K. Ogino, *Inorg. Chem.*, **28**, 3656 (1989).
16. B.T. Reagor and D.H. Huchital, *Inorg. Chem.*, **21**, 703 (1982).

17. K. Wieghardt, E. Schöffmann, B. Nuber and J. Weiss, *Inorg. Chem.*, **25**, 4877 (1986).
18. C.K. Johnson, ORTEP Report ORNL-3794, (Oak Ridge National Laboratory, Tennessee, 1985).
19. B.A. Frenz and J.A. Ibers, *Inorg. Chem.*, **11**, 1109 (1972).
20. Wada, N. Sakabe and J. Tanaka, *Acta. Cryst.*, **B32**, 1121 (1976).
21. M. Haque, C.N. Caughlan and K. Emerson, *Inorg. Chem.*, **9**, 2421 (1970).
22. R.D. Gillard and H.M. Irving, *Chem. Rev.*, **65**, 603 (1965).